Indoor Air, 2, 154-167 (1992)

Control of Airborne Particle Concentration and Draught Risk in an Operating Room

Qingyan Chen[1], Zheng Jiang, and Alfred Moser
Energy Systems Laboratory, Swiss Federal Institute of Technology, ETH-Zentrum, Zurich, Switzerland

Abstract

The influence of location of airborne particle source, ventilation rate, air inlet size, supply air velocity, air outlet location, and heat source on the distributions of airborne particle concentration and draught risk in an operating room is investigated. The investigation is carried out by using a flow program with the k-ε model of turbulence. Based on a standard case, five cases, each with one changed parameter, are computed, and the detailed field distributions of air velocity, temperature, airborne particle concentration, and draught risk are presented.

The parametric study concludes that, for a better air quality and thermal comfort, it is desirable to use a higher inflow rate, a larger inlet area, and a uniform velocity profile of supply air. Outlet location and heat source have little influence on the distributions of the particle concentration in the room. It has also been found that the distributions of particle concentration in the recirculating zone are very sensitive to the location of the particle sources.

KEY WORDS:
Hospital, Computation, Airflow, Concentration, Comfort, Design.

Manuscript received: 9 July 1991
Accepted for publication: 7 February 1992

[1] Present address: TNO Institute of Applied Physics (TPD), P. O. Box 155, 2600 AD Delft, Netherlands. Fax: + 31-15-692111

Introduction

The quality of indoor air in an operating room is an important component influencing the health and comfort of both the patient and the surgical team in the room. Woods et al. (1986) summarized that the infection of surgical wounds results from (1) self contamination by the patient through viscera or improper skin cleansing prior to surgery; (2) direct contact with unsterile instruments, contaminated surfaces or spread of droplets generated by hospital personnel in close contact with the patient; and (3) airborne droplet nuclei and dust which transmit microbiological agents to the surgical wound. Within an operating room, the surgical wound must be at least partially exposed. The airborne droplet nuclei and dust (particles) are particularly harmful to the health of the patient. The airborne particles may be controlled by properly ventilated air. At a certain activity level and with personnel in the operating room wearing a certain type of clothing, air velocity, air temperature, relative humidity, temperature stratification and turbulence intensity of air are all important parameters for thermal comfort. The influence of these parameters could vary under different ventilation systems. Thus, it is necessary to understand how airborne particles are transported, in order to control contamination, and to know how ventilation air is distributed, in order to guarantee optimal comfort.

A good ventilation system in an operating room is expected to reduce the concentration of airborne particles in room air to eliminate any possible infection in the operated area of the patient, and to provide an acceptable indoor climate for personnel and patients. Airborne particle transport and airflow pattern in an operating room depend, in general, on the following parameters: room geometry, equipment distribution, the number of persons in the room, airborne particle source location, air inflow rate, the position of air supply inlets and return outlets, and inlet characteristics. This paper studies the impact of these parameters on the airborne particle concentrations and draught risk in a typical operating room. Based on the predicted results, an optimum design of the ventilation system may be chosen from a number of possible alternatives, or the ventilation system may be improved to achieve lower concentration of airborne particles and thus a more comfortable environment in an existing operating room.

Research Method

Predictions of the indoor airflow pattern and airborne-particle concentrations are obtained by two main approaches: experimental investigation and numerical calculation. The most realistic information concerning indoor airflow is, in principle, given by direct measurement. Research in this field has been conducted mostly by experiments such as those of Woods et al. (1986), Zamuner (1986), and Hillerbrant and Ljungqvist (1990). The experimental measurements of the airborne particle concentration and thermal comfort in an operating room are, in most cases, expensive, and the experiment often does not present very detailed field results.

Due to the limitations of the experimental approach and to the rapid development of digital computer systems, numerical simulation of airflow and heat transfer in a room has been used extensively in recent years. In the numerical simulation, approximations are often required in the conservation equations of motion to make them solvable. For example, the details of turbulent flow are difficult to calculate, and engineers are mainly interested in the mean values. Therefore, one has to turn to so-called turbulence transport models to predict the mean values of flow variables. The turbulence transport models are still semi-empirically based and use a number of approximations. Using the k-ε model of turbulence (Launder and Spalding, 1974), encouraging results have been achieved in indoor airflow computation, as reviewed by Whittle (1986), Nielsen (1989), and Rhodes (1989). Therefore, the numerical technique with the k-ε model is employed in the present study.

In the present study, the modified k-ε model of turbulence is used (Chen et al. 1990). This model has been verified more suitable for predicting indoor airflow and heat transfer since the agreement between the computed and the measured results is very good. A more detailed description of the model and the comparison between the computed results and experimental data are given by Chen et al. (1990) and Borth (1990).

The airflow program developed by Rosten and Spalding (1987) has been employed to calculate air distribution. The computations involve the solution of three-dimensional equations for the conservation of mass, momentum (u, v, w), energy (H), contaminant concentrations ($C1$, $C2$), turbulence energy (k), and the dissipation rate of turbulence energy (ε). The governing equations of the model can be expressed in a standard form:

$$\mathrm{div}\,(\varrho \vec{V} \phi - \Gamma_\phi \,\mathrm{grad}\, \phi) = S_\phi \qquad (1)$$

where ϱ is the air density, $\vec{V}$ is the air velocity vector, Γ_ϕ is the diffusive coefficient, S_ϕ is the source term of the general fluid property, and ϕ can be any one of 1, u, v, w, k, ε, H, $C1$, or $C2$. When $\phi = 1$, the equation changes into the continuity equation.

Non-slip velocity and adiabatic boundary conditions are used in the numerical simulation. In the walls, the heat received due to radiation completely releases back to the room air due to convection. For the flow near the wall boundary layers, the wall function method is employed (Launder and Spalding, 1974).

Thermal comfort in a room is related to activity level, clothing type, air velocity, air temperature, relative humidity, temperature stratification, radiant temperature, radiant temperature asymmetry, and turbulence intensity. In an operating room, the activity level and clothing type are assumed to be the same under all the systems. With the same control strategy of the air-conditioning system and a large air change rate, the difference of relative humidity is small. Thus, the influence of relative humidity on thermal comfort may be negligible. The temperature difference between head (1.1 m) and ankle (0.1 m) in an operating room should be less than 2.5 °C, and the corresponding percentage of dissatisfied people will be less than 5% (Olesen et al. 1979). Furthermore, the effect of radiant temperature and radiant temperature asymmetry on thermal comfort can be neglected in an operating room. Therefore, the distributions of air velocity, air temperature, and turbulence intensity are important factors concerning thermal comfort in an operating room.

The mathematical model of draught risk, developed by Fanger et al. (1989), is used for the present study. The model includes the impact of air velocity, temperature, and turbulence intensity on thermal comfort, and predicts the percentage of dissatisfied people due to draught, PD, as:

$$PD = (34 - T_a)(V - 0.05)^{0.62}(3.14 + 0.37\,VI)\ (\%) \quad (2)$$

for $V < 0.05$ m/s insert $V = 0.05$ m/s, for $PD >$ 100% use $PD = 100\%$, where T_a is the local air temperature (°C), V is the mean velocity (m/s), and I is the turbulence intensity (%). The turbulence intensity I, is defined as the velocity fluctuation divided by the mean velocity. It is approximated as:

$$I = 100\,(2k)^{0.5} / V\ (\%) \quad (3)$$

where k is turbulence energy. T_a, V and k can be obtained from the airflow computation at each point of the flow field as mentioned above and therefore the PD distribution due to draught can be determined.

Case Set-up

Three air supply and return systems in use in operating rooms are considered. The first one supplies the air to the room vertically above the operating area from the ceiling to floor. This ventilation system creates a parallel and unidirectional flow above the operating area. The second ventilation system is "total mixing ventilation" in which air is supplied symmetrically from the ceiling or introduced through an inclined screen. In the total mixing ventilation system, the supply air is immediately mixed with the room air to achieve a uniform air distribution. With the third ventilation system, "displacement ventilation", the air is supplied at floor level and exhausted at ceiling level. The temperature of supply air is slightly lower than the room air temperature so that it stays at floor level before moving upward due to the buoyancy effect. The three ventilation systems used in operating rooms are compared in an experimental study carried out by Hillerbrant and Ljungqvist (1990).

In the present investigation, the first system is selected. For a typical operating room, geometry and equipment distribution are fixed. Therefore, the study concerns the influence of the following parameters on indoor airflow and airborne particle concentration in operating rooms: the location of airborne particle sources, air inflow rate, supply air velocity profile, air inlet size, the position of air return outlets, and heat source due to lighting and number of persons in the room.

In order to study the variation of the above parameters, a standard case (Case A) and five other cases are set up for an operating room. The operating room is assumed symmetrical in both geometry and

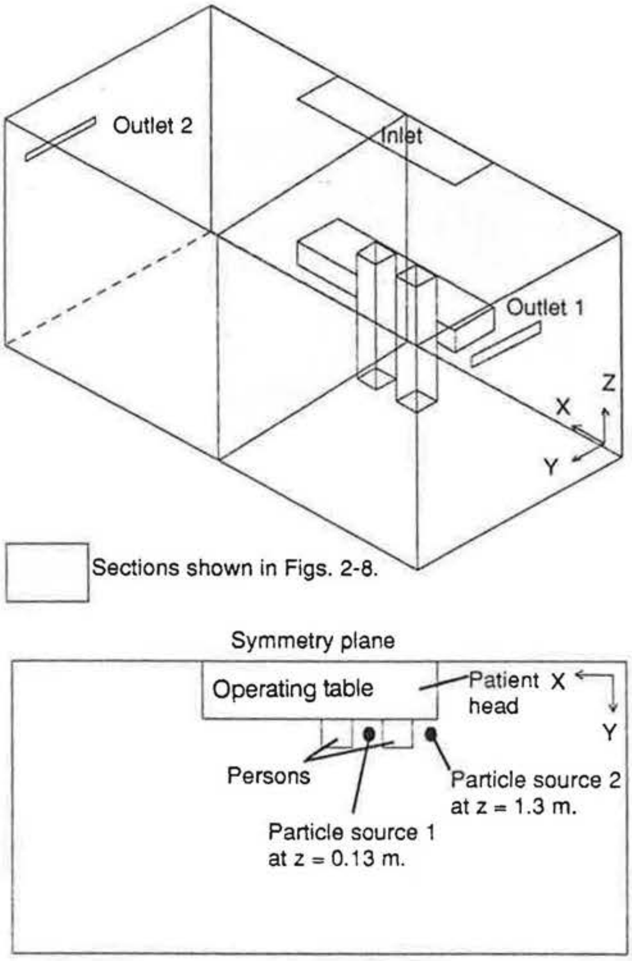

Fig.1 Sketch of the operating room.

boundary conditions, and computation is conducted for the half-room as shown in Figure 1. The geometry and boundary conditions for the half room in the standard case are as follows. The room is 6 m long, 3 m wide (whole room width is 6 m), and 3 m high with the symmetrical plane at y = 0. There are two outlets. The airflow rate through outlet 1, 1.0 m long and 0.14 m high, is fixed at 500 m^3/h. The length of another outlet is 1.0 m and height 0.09 m. The inlet is a simple slot in the ceiling with a size 2.3 m long and 0.6 m wide. The total air supply to the half room is 1500 m^3/h corresponding to 28 ach (air change per hour). The supply air velocity is assumed to be uniformly distributed over the entire area of the supply opening. For the standard case, the air velocity is 0.3 m/s. The supply air temperature is 20.0 °C. The filter in the inlet is assumed to be well maintained so that there is no airborne particle from the supply air. In the half room, two operating persons emitting 75 W convective heat each stand near the operating table. The heat from the

Table 1 The difference in boundary conditions between the standard case and the other cases.

Case	Supply airflow m^3/h	Inlet size $m \times m$	Velocity profile	Outlet location	Heat source W
A	1500	0.6 × 2.3	Uniform	Upper	680
B	1000	"	"	"	"
C	1500	1.2 × 2.3	"	"	"
D	"	0.6 × 2.3	Non-uniform	"	"
E	"	"	Uniform	Lower	"
F	"	"	"	Upper	1100

operation lights is 150 W and from other lights on the ceiling and equipment 380 W. An assumed 20% of the total heat is radiative heat that is absorbed uniformly by the walls and then released to the room air by convection between the walls and room air. This means that the boundary conditions of heat transfer for all the walls, ceiling and floor are set to be adiabatic. However, the radiation between the operation lights and the patient is not taken into account to simplify the problem. With the consideration of radiation, the surface temperature of the patient will be higher than that without radiation. On the other hand, the radiation from the patient to the surrounding surface will be higher too. The surface temperature of the patient with the consideration of radiation will only be slightly higher and will not result in a notable influence on the air distribution. Therefore, the simplification would be acceptable.

There are two airborne particle sources in the room as shown in Figure 1. One is located at x = 2.55 m, y = 0.75 m, and z = 0.13 m and the other at x = 2.0 m, y = 0.75 m, and z = 1.3 m. Particle source 1 is at one of the doctors' ankle level and source 2 at the level of an equipment table. The emission rate of the particle sources is normalized to 1 particle/s. The airborne particles are with a turbulent Schmidt number of 1. There is no relative velocity between the particles and the air carrying the particles.

Results

This section presents the computed field distributions of airborne particle concentration and airflow patterns under different boundary conditions (parameters). The boundary conditions for the standard case have been described above. The differences in boundary conditions between the standard case and the other cases are summarized in Table 1.

The computations are performed for the operating room with and without the aerodynamic blockage for the operating table and personnel. For each parameter, the simulations were done for at least three values. However, only the typical results for the room with aerodynamic blockages are presented in this paper.

Case A: Standard Case

The computed field distributions of air velocity, temperature, the concentration of particles 1 and 2 concentration for the standard case (Case A) are shown in Figure 2. The velocity vectors are shown in two vertical mid-sections of the room (the right one is in the symmetric plane). This ventilation system presents a vertical, unidirectional flow above the operated area. The air temperature distributions are also illustrated in the two mid-sections. Since the air change rate is rather high, the air temperature difference in the room is accordingly small. The higher vertical temperature gradient near the ceiling is due to the heat source from the lights. Two airborne particle sources are assumed to be placed in two different positions. The concentration contours are plotted in two sections: one in the symmetric plane (on the right) and the other at the section via the sources (on the left). The results show that the particle concentration in the operated area is "zero". Since there are very large numbers of particles generated at each of the source locations considered and there are probably many other sources as well, including particles that penetrate the filter in the ceiling, the term "very small" will be used to replace "zero", an ambitious term. The very small particle concentration implies that the air quality in the operated area is controlled only by the supply air. However, in the rest of the room (recirculating zone), the transportation of the particles depends on the source location and airflow patterns.

The field distributions of percentage of dissatisfied people due to draught are illustrated in Figure 3. In most of the room, the percentage is less than 20%. This value is acceptable from the viewpoint of thermal comfort.

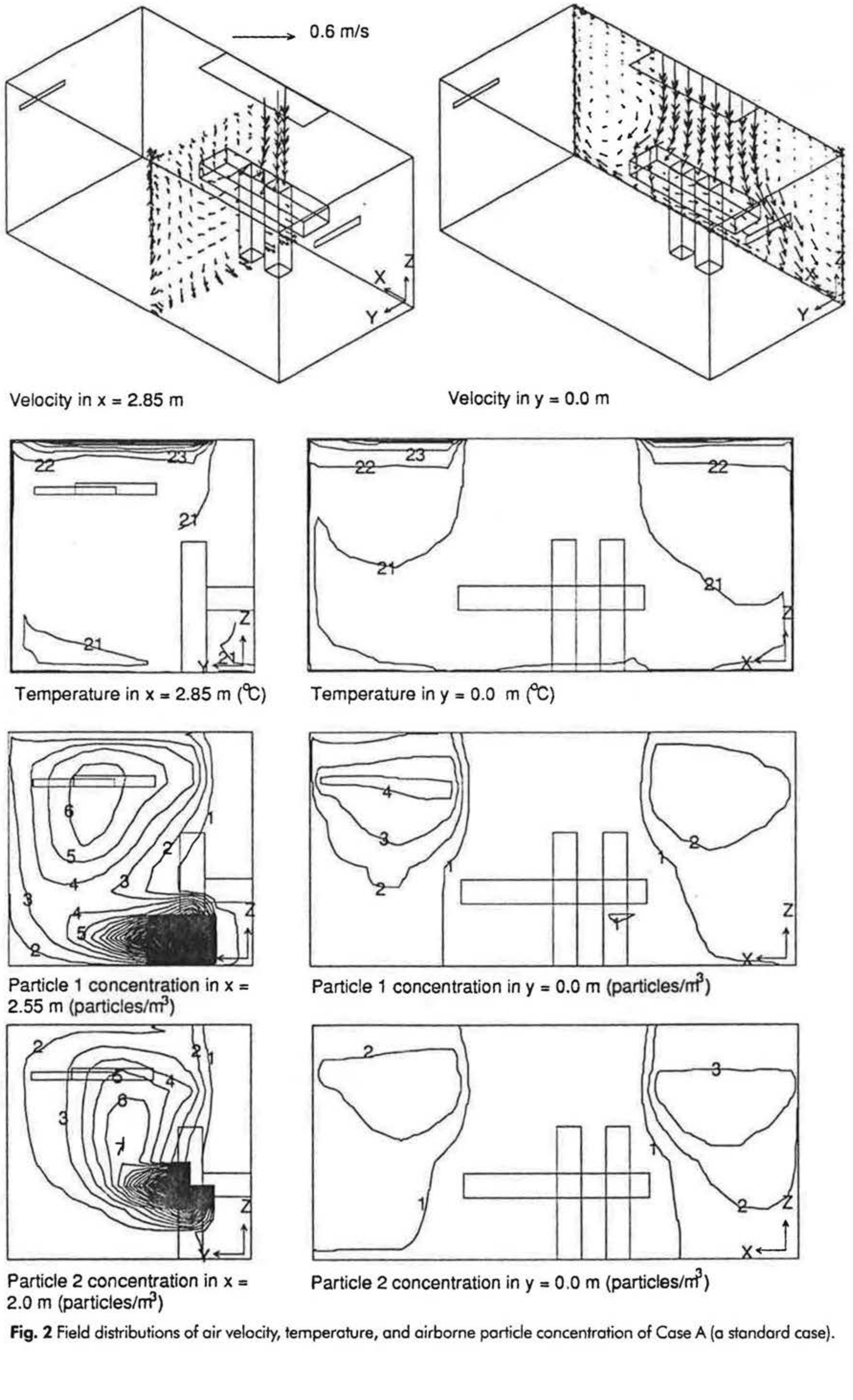

Fig. 2 Field distributions of air velocity, temperature, and airborne particle concentration of Case A (a standard case).

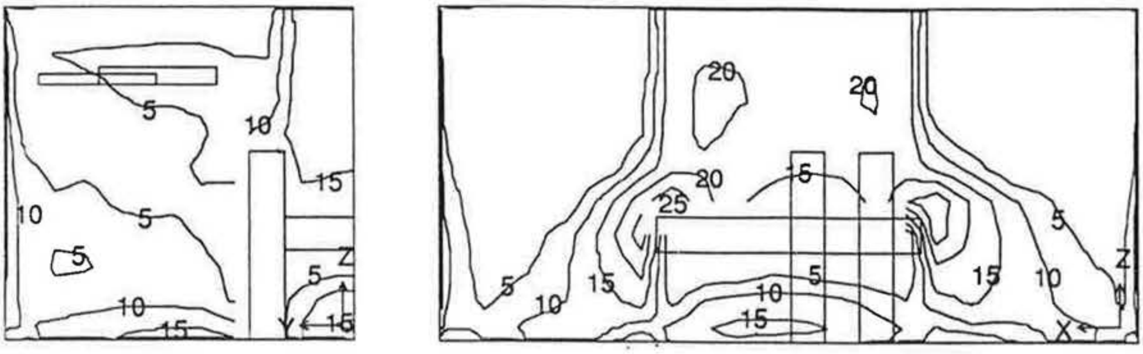

PD in x = 2.85 m　　PD in y= 0.0 m

Fig. 3 Field distributions of percentage of dissatisfied people due to draught (%).

Case B: with a Different Air Inflow Rate

This subsection discusses the influence of air supply rate on the distributions of airborne particle concentration and draught risk. The air inflow rate, which is 1500 m^3/h for the half room in the standard case, is reduced to 1000 m^3/h for Case B. The other boundary conditions are the same.

Figure 4 shows the computed field distributions of air velocity, temperature, and the concentration of particles 1 and 2. The airflow patterns of Cases A and B are very similar while the velocity magnitude of Case B is smaller. As a result, the maximum PD in the operated area for Case B is 6% smaller than that for Case A.

Since the inflow rate is lower, the average room air temperature is 0.8 °C higher. But this temperature difference contributes very little to draught risk.

Comparing the concentration distributions of the airborne particles 1 and 2 in Cases A and B as shown in Figures 2 and 4, it is obvious that the higher the inflow rate, the lower the particle concentration. In the operated area, the concentration for both cases is very small. This indicates that it may be unnecessary to supply such a large amount of air. However, the concentration in the recirculating zone depends very much on the inflow rate. The higher concentration in the recirculating zone in Case B may be a risk of infection. The air inflow rate does not have a significant impact on the concentration of particle 1. The impact is considerably larger for particle 2, especially on the right side at section y = 0.0 m.

Case C: with a Different Air Inlet Size

The results of Cases A and B show that the air quality in the operated area is mainly controlled by the ventilated air. The air inflow rate has very little influence on the air quality in the operated area. However, since the air quality in the recirculating zone is also important for reducing possible risk of infection, the amount of supply air must not be too small to achieve better air quality in the zone. With a certain amount of supply air, it may be a good solution to increase the inlet size so that a larger clean area under the inlet may be created.

In order to study the effect of inlet size on the airborne particle concentrations and airflow patterns, the inlet size, which is 2.3 m long and 0.6 m wide for the standard case, is increased to 2.3 m long and 1.2 m wide for Case C as shown in Figure 5. The other flow boundary conditions for Case C are the same as for Case A.

Since the inlet size of Case C is twice as large as for Case A, the inlet velocity is reduced to one half. The airflow patterns between the two cases are similar although there are some differences such as in the region about 1 m above the patient's head (see Figures 2 and 5). In the region, the buoyancy effect is strong, and forms a large recirculation. In addition, the air velocities for Case C are smaller. Thus, the maximum PD for Case C is about 5% smaller than that for Case A.

The temperature distributions of the two cases, illustrated in Figures 2 and 5, do not show any significant differences. The inlet velocity for the operating room with this ventilation system is relatively small. Hence, it will not disturb the airflow pattern in the room due to its low momentum. Because the air inflow rate of the two cases is the same, the temperature distributions may be similar.

As expected, Case C does have a larger clean area above the operating table because of its larger inlet size. This can be seen by comparing the concentration distributions of Cases A and C. However, the strong recirculation above the patient's head brings the contaminated air that results in a higher concen-

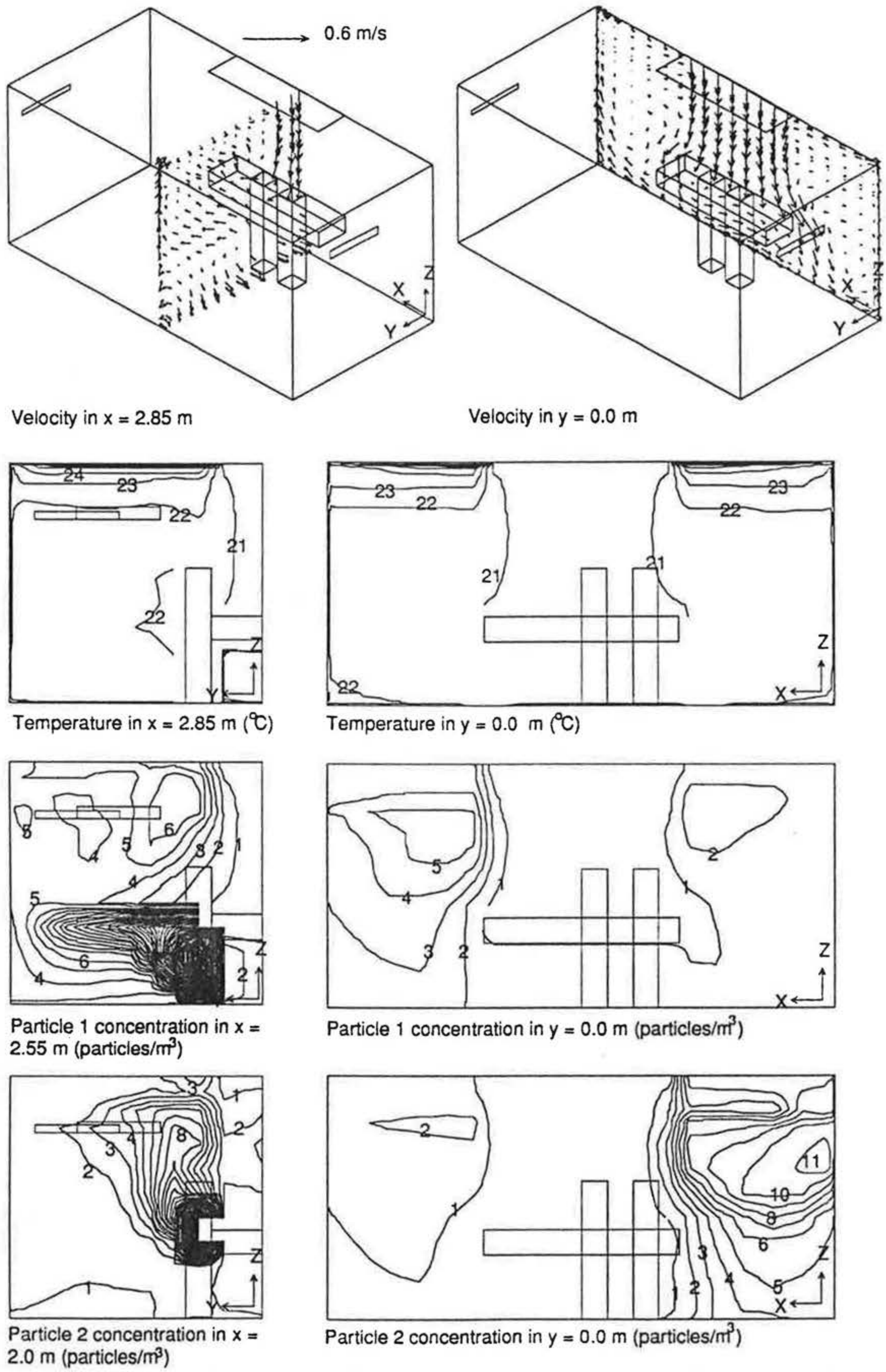

Fig. 4 Field distributions of air velocity, temperature, and airborne particle concentration of Case B (a case with a different air inflow rate).

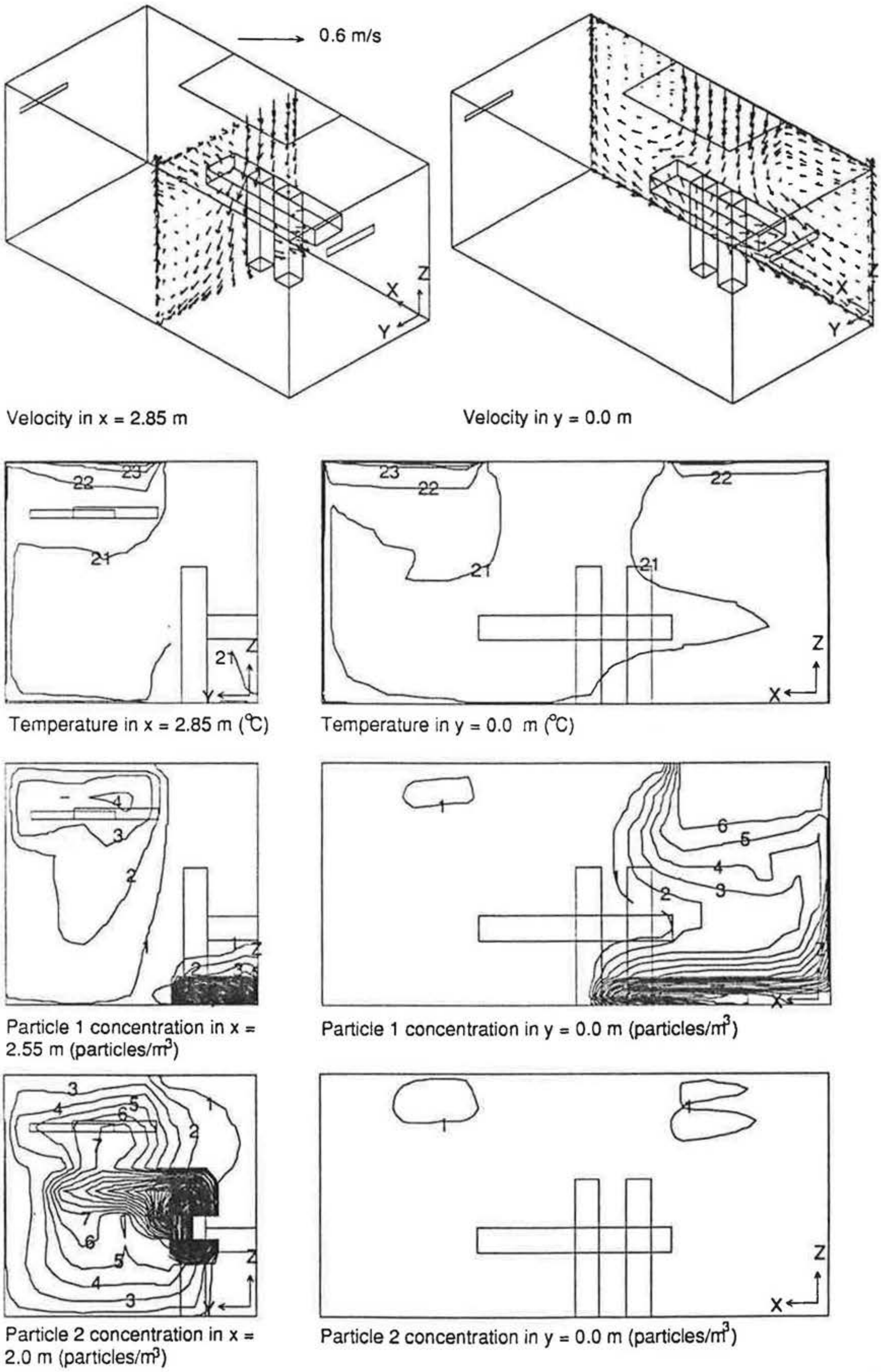

Fig. 5 Field distributions of air velocity, temperature, and airborne particle concentration of Case C (a case with a different air inlet size).

tration of particle 1 in that region. Our other computed results, although not shown here, suggest that it is desirable to increase both inlet length and width but the inlet area should not exceed double the inlet area of Case A for the conditions discussed.

However, from Figures 2 and 5, one cannot judge which inlet size would create better air quality. The particle concentrations are very different to the airflow patterns. The computed results without the aerodynamic blockages for the table and personnel that are not presented here show that the particle concentrations are similar under different inlet sizes. This implies that those aerodynamic blockages are important for indoor air distribution.

Case D: with a Different Velocity Profile of Supply Air

The air recirculation could be rather strong in an operating room. This recirculation may bring contaminated air to the operated area as observed in Case C. Since the most important issue in designing the ventilation system in an operating room is to ensure a clean environment in the operated zone, it is necessary to prevent such a recirculation. Using different velocity profiles of supply air may be useful.

Case D as shown in Figure 6 is designed to test the influence of the velocity profile of supply air on airborne particle concentrations and airflow patterns. In Case D, the inlet is divided into two zones. The outer zone has a velocity of 0.4 m/s and the inner zone 0.15 m/s (the supply air velocity for Case A is 0.3 m/s). The outer zone forms an air curtain that may prevent contaminated air from entering the inner zone. All other boundary conditions for Case D, including the air inflow rate, are the same as for Case A.

There are recirculations in the operated area in Case D as shown in Figure 6. The airflow is no longer unidirectional, and airborne particles may be carried from the operating table to the operated area. Therefore, this kind of velocity profile of supply air is not recommended. The difference in the distribution of air temperature and concentration of particles 1 and 2 between Cases A and D are similar. Case D does not show improvement in air quality. On the contrary, it results in a 3% higher PD value than in Case A under the outer zone of the inlet.

Case E: with a Different Air Outlet Location

Case E is used to examine the impact of outlet location on airborne particle concentration and airflow pattern. As shown in Figure 1, there are two outlets in the half operating room. The location of outlet 1 cannot be changed, because it is the inlet for the adjacent room. The other outlet on the rear wall (outlet 2) is moved to the floor level in Case E as shown in Figure 7. All other boundary and geometry conditions for Case E are the same as those for Case A.

As illustrated in Figure 2 (for Case A) and Figure 7 (for Case E), the location of an air exhaust outlet has very little influence on room airflow pattern. The outlet position may be an important parameter in determining the mean air temperature and particle concentration, but not in the present study. Since the vertical gradients of the air temperature and particle concentrations along the rear wall are small, the change of outlet location from Cases A to E does not make a significant contribution to the mean air temperature and particle concentration, and the discrepancies of the distributions of air temperature and particle concentration between the two cases are negligible.

The distributions of PD between Cases A and E are similar. The difference is less than 1% according to the numerical results.

Case F: with a Different Heat Source

In an operating room, the strength of the heat source can be different from one operation to another. Case F is used to analyse the influence of the output power of heat source on airborne particle concentration and airflow patterns. The total heat source in Case F is increased from 680 W in Case A (operation light is 150 W, other lights on the ceiling except at the inlet region 380 W, and 2 persons 150 W) to 1100 W (operation light is 150 W, equipment around the operating table 150 W, other lights on the ceiling except at the inlet region 500 W, and 4 persons 300 W). The heat source is the only difference in the flow and thermal boundary conditions between Cases A and F.

The computed field distributions of air velocity, temperature, and the concentration of particle 1 and 2 for Case F are shown in Figure 8. Although the heat source in Case F is almost twice as much as that in Case A, the velocity distributions in the operated area are the same. This again confirms that the airflow in the operated area is mostly controlled by the ventilated air. There are some differences in the rest of the room, and the air velocities are smaller in Case F.

The vertical temperature gradient and average room air temperature in Case F are higher than in

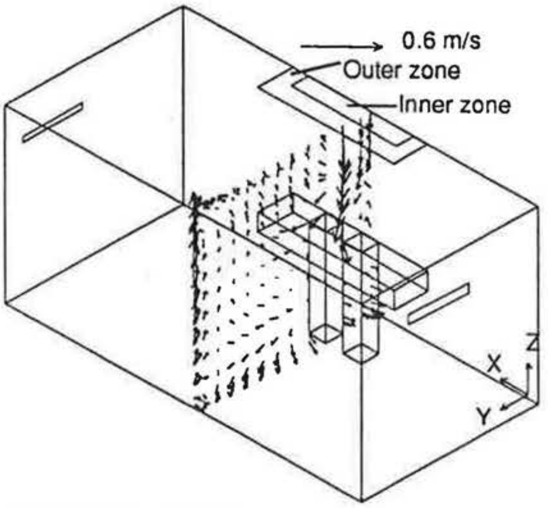

Velocity in x = 2.85 m

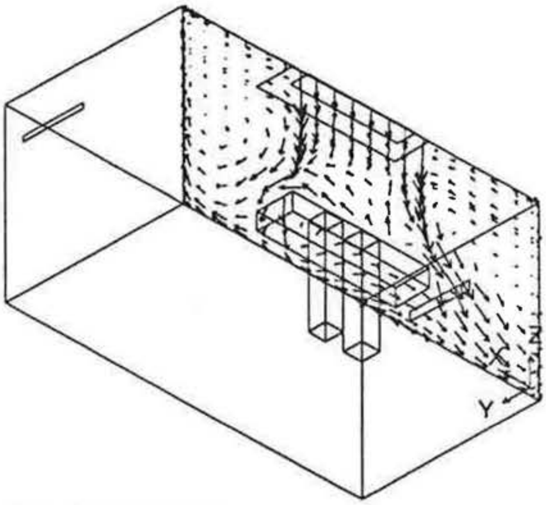

Velocity in y = 0.0 m

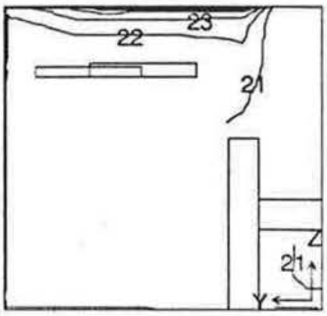

Temperature in x = 2.85 m (℃)

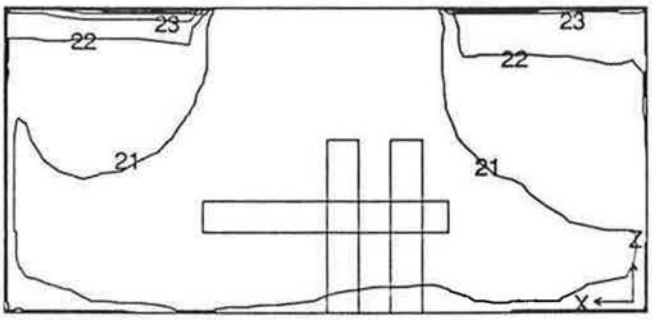

Temperature in y = 0.0 m (°C)

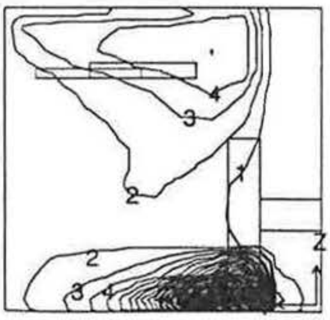

Particle 1 concentration in x = 2.55 m (particles/m³)

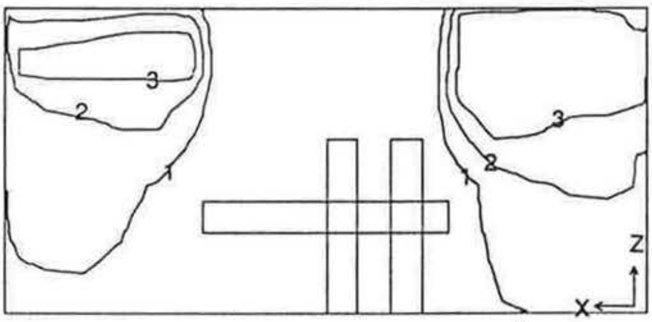

Particle 1 concentration in y = 0.0 m (particles/m³)

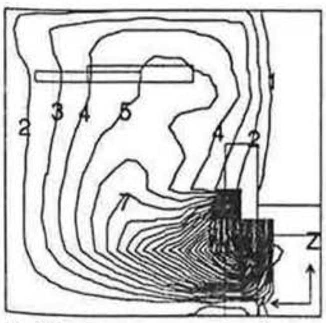

Particle 2 concentration in x = 2.0 m (particles/m³)

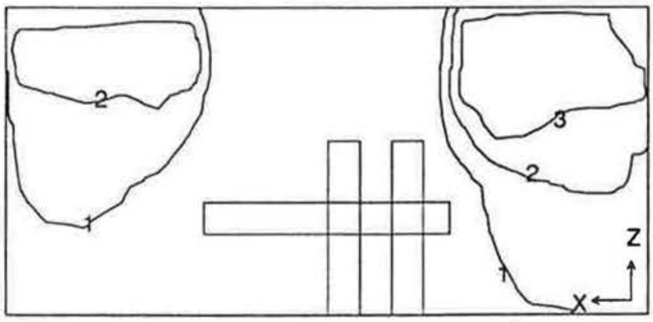

Particle 2 concentration in y = 0.0 m (particles/m³)

Fig. 6 Field distributions of air velocity, temperature, and airborne particle concentration of Case D (a case with a different velocity profile of supply air).

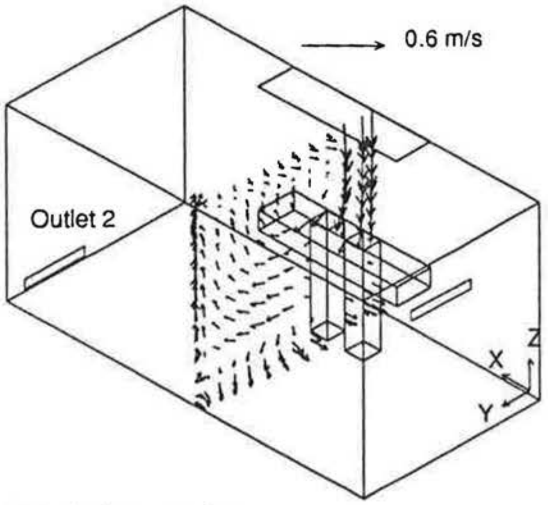

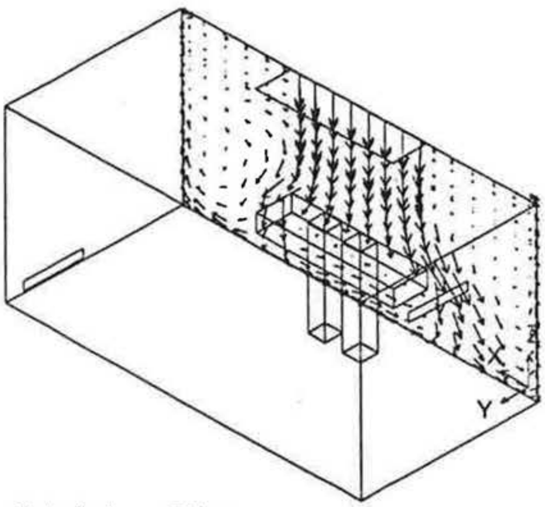

Velocity in x = 2.85 m

Velocity in y = 0.0 m

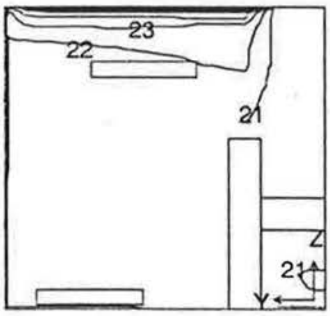

Temperature in x = 2.85 m (°C)

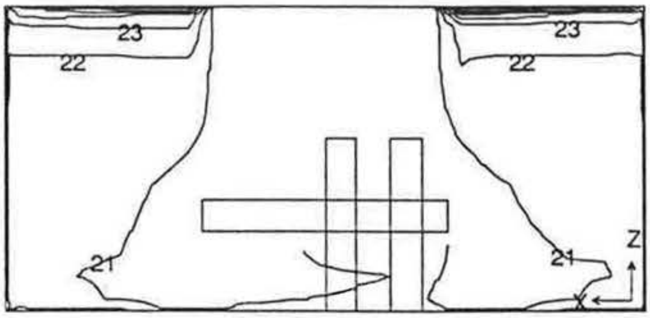

Temperature in y = 0.0 m (°C)

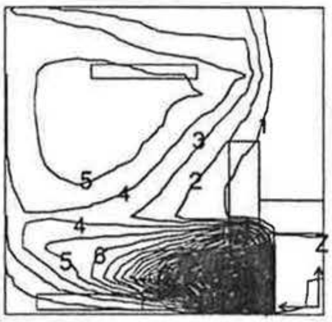

Particle 1 concentration in x = 2.55 m (particles/m³)

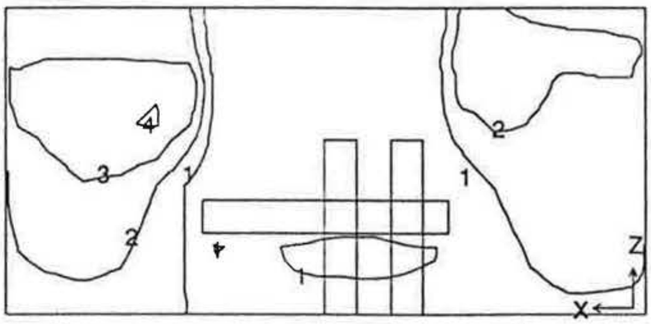

Particle 1 concentration in y = 0.0 m (particles/m³)

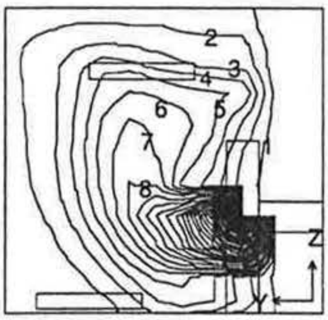

Particle 2 concentration in x = 2.0 m (particles/m³)

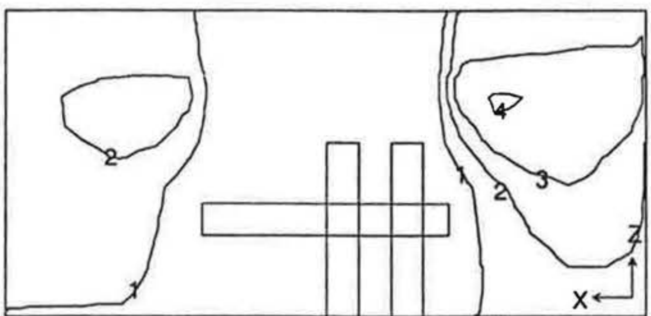

Particle 2 concentration in y = 0.0 m (particles/m³)

Fig. 7 Field distributions of air velocity, temperature, and airborne particle concentration of Case E (a case with a different air outlet location).

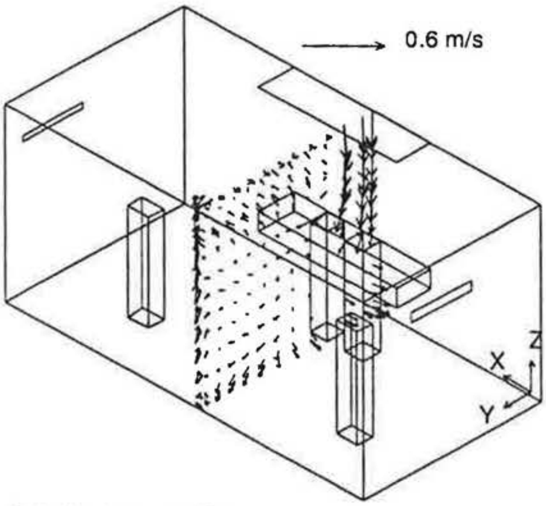

Velocity in x = 2.85 m

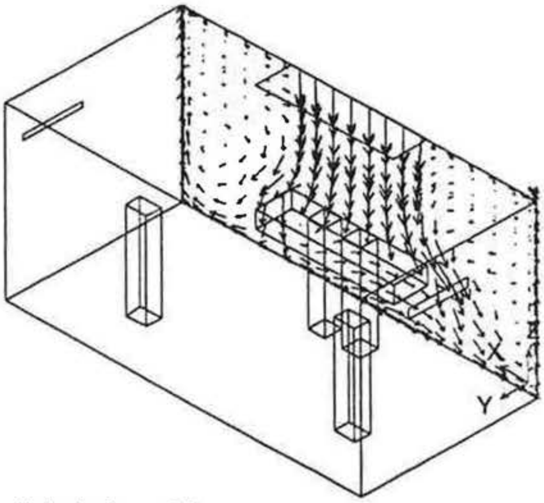

Velocity in y = 0.0 m

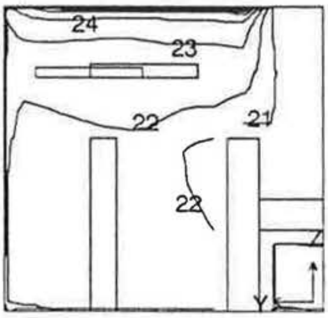

Temperature in x = 2.85 m (℃)

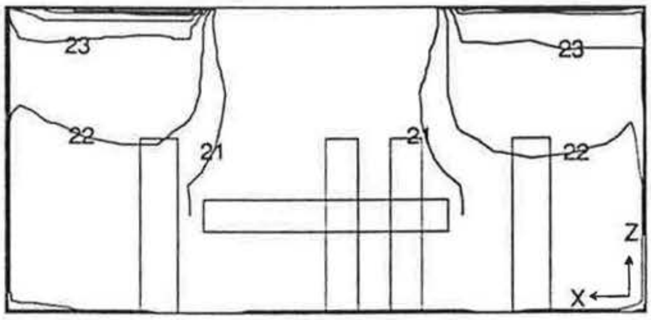

Temperature in y = 0.0 m (℃)

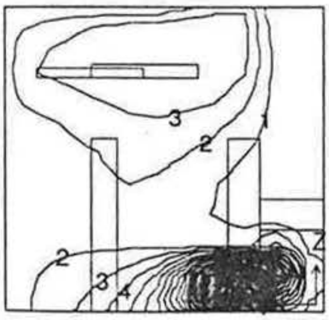

Particle 1 concentration in x = 2.55 m (particles/m^3)

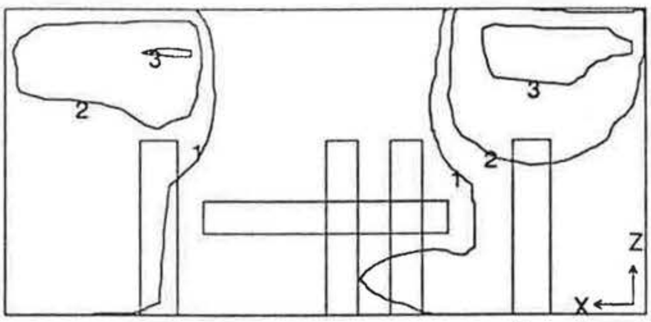

Particle 1 concentration in y = 0.0 m (particles/m^3)

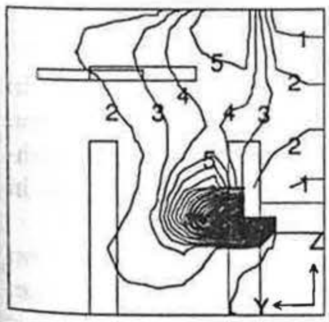

Particle 2 concentration in x = 2.0 m (particles/m^3)

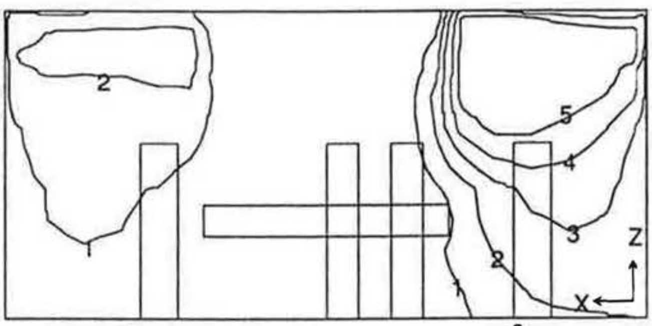

Particle 2 concentration in y = 0.0 m (particles/m^3)

Fig. 8 Field distributions of air velocity, temperature, and airborne particle concentration of Case F (a case with a different heat source).

Case A because of the higher heat source. But the temperature difference between head and ankle levels is less than 1 °C, which should have no impact on thermal comfort.

The concentration of particle 1 in Case F is slightly lower than in Case A, while the concentration of particle 2 is slightly higher. The results from another case, not included in the present study, indicated that the influence of heat source is extremely large if a particle source is located above the heat source.

Discussion

The computations presented in this paper are considered convergent if the sum of the absolute residual for mass continuity in all the cells is less than 0.01% the total mass inflow. Since it is more difficult to control the energy balance, the computations are terminated when the sum of the absolute residual for energy balance in all the cells is smaller than 0.1% the total energy in the mass inflow. With such a numerical accuracy, the CPU time in CRAY XMP super computer is about 1 hour for a case. The same computation could be done on a work station but the CPU time could be as much as two days.

For an experienced user of a commercial computational fluid dynamics (CFD) program, it may take one week to set up and get correct results for the first case. For remaining cases, it is easy to modify the boundary conditions in a computer simulation. With reasonably good post-processing software, it takes less than a day to plot the results into the figures in the sections of interest. This implies that it should be possible to use the present approach in the design phase. However, the designer should have a good knowledge of computational fluid dynamics. It may take up to 6 months for a beginner to use a CFD program for his problem with confidence.

Numerical diffusion can play an important role in the transport of a contaminant. Therefore, sufficient grid cells must be used to avoid numerical diffusion. In the present study, if the grid cells are further doubled, the results in most cells do not vary much (less than 2%). This numerical diffusion in the investigation is smaller than the magnitude of the turbulent diffusion.

It should be noted that the particle transport is simulated by a concentration conservation equation. The shear stress caused by the particles, the gravitational setting and electrostatic force effect are not taken into account. This assumes that the particles follow the flow path without deviation due to momentum differences. This is valid only for gas-phase contaminants. The effect of different particle size on its transport should be studied further.

The calculations are made with fixed human objects. In reality, the occupants in the operating room may move. This means the contaminant source location may change and the distribution of the contaminant, as well as the flow field, may be different. A further study on the movement of the occupants on the flow and contaminant concentration is necessary.

Conclusions

The field distributions of air velocity, temperature, the concentration of airborne particles, and draught risk are studied by numerical simulation with the k-ε model of turbulence. This method is very powerful for the parametric study of flow and thermal boundary conditions.

The influences of the source locations of airborne particles, supply-air inflow rate, air inlet size, supply-air velocity, air outlet location, and heat source on the distributions of airborne particle concentration and draught risk for an operating room are investigated. The air is supplied to the room in a parallel manner through the operating area from ceiling to floor. The following facts have been found from the case study:

- The concentration of airborne particles is very small in the operating area regardless of the location of the two particle sources in the present study. The air quality in the operating area is controlled only by the supply air. However, the particle concentration in the recirculating zone is strongly dependent on the location of the particle sources.
- With different ventilation rates, the airflow patterns are similar in the room. The higher the inflow rate, the lower the particle concentration in the recirculating zone. The particle concentration in the operating area remains very small. A higher inflow rate results in a higher draught risk in the room.
- The area with very small particle concentration above the operating table is a little smaller than the inlet area. When the inflow rate is fixed, it is desirable to use a large inlet for this type of ventilation system. A larger inlet implies a lower supply velocity which is better for thermal comfort.

- A uniform velocity profile of supply air seems to be better for the operating room studied, since a complex velocity profile of supply air velocity may cause recirculation within the operating area.
- The outlet location in the operating room has very little influence on the concentration of airborne particles and airflow pattern.
- A higher heat source in the room does not have a significant influence on the distributions of particle concentration as long as the particle source is not placed right above the heat source. A higher heat source leads to a higher vertical temperature gradient and higher room air temperature. But the influence of heat source strength on thermal comfort is negligible.

Acknowledgments

The authors would like to thank Meierhans & Partner AG in Switzerland for their partial financial support of the investigation.

References

Borth, J. (1990) "Numerical simulation of airflows in rooms", *ERCOFTAC Bulletin*, 5, 9-14.

Chen, Q., Moser, A. and Huber, A. (1990) "Prediction of buoyant, turbulent flow by a low-Reynolds-number k-ε model", *ASHRAE Transactions*, 96(1), 564-573.

Fanger, P.O., Melikov, A.K., Hanzawa, H. and Ring, J. (1989) "Turbulence and draft: the turbulence of airflow has a significant impact on the sensation of draft", *ASHRAE Journal*, 31(7), 18-23.

Hillerbrant, B. and Ljungqvist, B. (1990) "Comparison between three air distribution systems for operating rooms", In: *Proceedings of ROOMVENT '90*, Oslo, NORSK VVS, pp.[illegible].

Launder, B.E. and Spalding, D.B. (1974) "The numerical computation of turbulent flows", *Computer Methods in Applied Mechanics and Engineering*, 3, 269-289.

Nielsen, P.V. (1989) "Progress and trends in air infiltration and ventilation research", In: *Proceedings of the 10th AIVC Conference*, Dipoli, Air Infiltration and Ventilation Centre, pp.[illegible].

Olesen, B.W., Scholer, M. and Fanger, P.O. (1979) "Discomfort caused by vertical air temperature difference", In: *Proceedings of Indoor Climate*, Copenhagen, Danish Building Research Institute, pp.531-539.

Rhodes, N. (1989) "Prediction of smoke movement: an overview of field models", *ASHRAE Transactions*, 95(1), pp.868-877.

Rosten, H.I. and Spalding, D.B. (1987) *The PHOENICS Reference Manual*, Version 1.4, London, CHAM Ltd. (Report No TR200).

Whittle, G.E. (1986) "Computation of air movement and convective heat transfer within buildings", *International Journal of Ambient Energy*, 3, 151-[illegible].

Woods, J.E., Braymen, D.T., Rasmussen, R.W., Reynolds, G.L. and Montag, G.M. (1986) "Ventilation requirements in hospital operating rooms-part 1: control of airborne particles", *ASHRAE Transactions*, 92(2), [illegible]-426.

Zamuner, N. (1986) "Operating room environment with turbulent airflow", *ASHRAE Transactions*, 92(2A), 343-349.